Insights through dynamic analysis of structures at liquefied sites

J.D. Bray & R. Luque

Department of Civil & Environmental Engineering, University of California, Berkeley, CA USA.

2017 NZSEE Conference

ABSTRACT: Several buildings in Christchurch settled differentially and were damaged as a result of soil liquefaction during the Canterbury earthquake sequence. Nonlinear effective stress soil-structure interaction analyses were performed to gain insights regarding the mechanisms contributing to building movements. Shear strains in the foundation soils developed due to shaking-induced ratcheting of buildings into cyclically softened soil or due to a transient loss of bearing due to soil softening in several cases. This led to a significant part of the liquefaction-induced building settlement. Damaging building settlement due to volumetric strains in the foundation soils were largely due to liquefaction of shallow soils, if they were present. The dynamic soil-structure interaction analyses captured these mechanisms of nonlinear soil response. However, the influence of the loss of ground due to sediment ejecta, which was another important factor in some cases, was not captured with this continuum based approach. Engineers should employ simplified procedures and judgment to assess this mechanism.

1 INTRODUCTION

Several buildings in Christchurch settled differentially and were damaged as a result of soil liquefaction during the 2010-2011 Canterbury earthquake sequence. The state-of-the practice still largely involves estimating building settlement using empirical procedures developed to calculate post-liquefaction, one-dimensional (1D), consolidation settlement in the free-field away from buildings. These free-field analyses cannot possibly capture shear-induced deformations in the soil beneath shallow foundations. Liquefaction-induced displacement mechanisms are shown in Figure 1. Liquefaction-induced building movements are often controlled by shear-induced ground deformations as a result of soil-structure interaction (SSI)-induced ratcheting and bearing capacity movements (e.g., Dashti and Bray 2013). The removal of materials beneath a structure due to the formation of sediment ejecta can also be important. Volumetric-induced ground deformations resulting from localized partial drainage, sedimentation, and post-liquefaction reconsolidation may also contribute to the settlement. 1D empirical procedures can only capture the settlements as a result of the cumulative effect of volumetric strains related to sedimentation and post-liquefaction reconsolidation mechanisms.

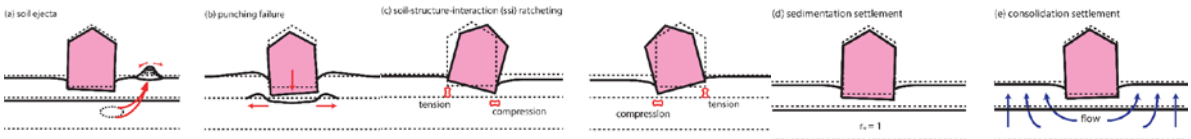

Figure 1. Liquefaction-induced displacement mechanisms: (a) ground loss due to soil ejecta; shear-induced settlement from (b) punching failure, or (c) soil-structure-interaction (SSI) ratcheting; and volumetric-induced settlement from (d) sedimentation, or (e) post-liquefaction reconsolidation.

Thus, nonlinear effective stress fully coupled dynamic soil-structure interaction (SSI) analyses are required to capture the phenomena and gain valid insights. Numerical analyses have been used by researchers to replicate the measured responses of the ground or structures during physical experiments, which are commonly centrifuge tests (e.g., Karimi and Dashti 2016). Few papers describe the back-analysis of liquefaction-induced building movement case histories. Two cases from a recent study of multi-story office buildings damaged in Christchurch are summarized in this paper.

2 INPUTS TO DYNAMIC SSI ANALYSES

2.1 Earthquake ground shaking

Ground shaking was recorded at four strong motion stations within the Central Business District (CBD). The 22 February 2011 Christchurch M_W 6.2 earthquake produced the most intense ground shaking in the CBD, because the source-to-site distances (R) were only 3-6 km. Its peak ground acceleration (PGA) values were twice those recorded during the larger, but more distant 4 September 2010 Darfield M_w 7.1 event (R = 18-20 km). This paper focuses on the seismic performance of two multi-story office structures supported on shallow foundations during these earthquakes.

Free-field ground surface median PGA values at the building sites were estimated using Bradley (2014) to be 0.22 g and 0.45 g for the Darfield and Christchurch earthquakes, respectively. The estimated median PGAs values were consistent with the PGA values recorded at the four CBD strong motion stations surrounding the sites (Bray et al. 2014). Liquefaction was not observed at these stations for the Darfield event, but it was observed at some of the stations for the Christchurch event; however, the PGA values occurred before liquefaction effects are observed in the records so they were are not likely influenced by liquefaction.

There are no "outcropping rock" site recordings to use directly in the dynamic SSI analysis. Additionally, the Canterbury basin is hundreds of meters deep, and most of its soil layers are not well characterized. There is a significant impedance contrast between the near surface soils and the pervasive, dense Riccarton Gravel layer, which is at a depth of about 20-24 m in the CBD. Thus, recorded ground motions at shallow, stiff (non-liquefiable) soil sites west of the CBD were used by Markham et al. (2016) to deconvolve "within" motions for the top of the dense Riccarton Gravel layer. The deconvolved Riccarton Gravel motions were modified to consider the differences of the rupture distance (R_{rup}) and the stiffness of the Riccarton Gravel between the deconvolution sites and the CBD sites as described by Markham et al. (2016). The modified "within" Riccarton Gravel motions were assigned at the rigid base of the numerical model as input motions.

2.2 Calibration of the soil constitutive model and dynamic analysis

The PM4Sand Version 3 (Boulanger and Ziotopoulou 2015) constitutive model was used to capture the cyclic response of sandy soils. PM4Sand model parameters were developed using best-estimated median values of unit weights (γ), relative densities (D_r), and shear wave velocities (V_s). The use of median values of relative density is consistent with the recommendations of Boulanger and Montgomery (2016) who found characteristic values for uniform models to be within the 30^{th} and 70^{th} percentiles when estimating liquefaction-induced ground displacements. Median values of these parameters were obtained through conventional correlations with the CPT (e.g., Robertson 2010), and the McGann et al. (2014) Christchurch-specific correlation for V_s, which then was used to obtain the normalized shear modulus (G_o). Additional parameters found from laboratory testing (Markham et al. 2016b and Taylor 2015) include critical state line parameters (Q = 8.0 and R = 1.0), critical state friction angle (φ_{cv}), bounding surface parameter (n_b) and maximum and minimum void ratios (e_{max} and e_{min}). Keeping these parameters fixed and using the confining pressure of the different units, element tests were modelled in FLAC 2D (Itasca, 2011) and the contraction rate parameter (h_{po}) was varied to obtain the cyclic resistance ratio (CRR) at 15 cycles obtained from the advanced laboratory testing or the Boulanger and Idriss (2016) simplified liquefaction procedure. Laboratory test specimens were of high quality as noted by Markham et al. (2016b) using the Dames & Moore hydraulic fixed piston sampler or by Taylor (2015) using the Gel-push sampler. Thus, careful sampling and testing are required to obtain reliable lab test results. The soil parameter values selected for the PM4Sand model used for sandy soils at building sites are provided in Table 1. Default PM4Sand model parameter values were used for the other model parameters not shown in Table 1.

A representative comparison of the numerical simulations and the laboratory test results are presented in Figure 2. The key aspects of nonlinear soil response due to excess pore water pressure generation are captured by the PM4Sand model. Additionally, the number of cycles to reach liquefaction

triggering were reasonable. Free-field site responses of the sites without the presence of the buildings were also performed to ensure the ground motions calculated at the ground surface of these sites compared favourably with the ground motions recorded at the nearby strong motion sites and the soil layers with low factor of safety estimated from simplified procedures developed significant excess pore water pressures and shear strains in the numerical analyses.

Table 1. PM4Sand model parameters for cohesionless soils at FTG-7 and CTUC building sites.

Parameter	CTUC					FTG-7				Source
	Fill	SM/ML**	SP/GP	SP/SM	SP	Fill	SM/ML**	SP/SM	SP	
γ (kN/m^3)	17	16.6	19.7	19.3	20.3	18.8	17.3	18.8	20.3	CPT*
D_r (%)	50	35-45	85	65	85	63	35-40	63	89	CPT*
G_O	500	350-450	1500	900	2000	400	300-400	760	1350	CPT*
h_{po}***	1.0	1.2 (3.5)	3	0.3	7.0	1.2	2.2 (0.15)	0.55	20	Calib.
φ_{cv}	35	35	35	35	35	35	35	35	35	T(15)
Q	8	8	8	8	8	8	8	8	8	M(16b)
R	1	1	1	1	1	1	1	1	1	M(16b)
n_b***	1.4	1.4 (0.15)	1.4	1.4	1.4	0.8	0.8	0.6	0.6	T(15)
e_{max}	1.3	1.25	1.1	1	1	1.2	1.3	1	1	T(15)-CPT*
e_{min}	0.6	0.6	0.6	0.6	0.6	0.6	0.6	0.6	0.6	
k (m/s)	1.1e-5	2.0e-6	3.8e-4	4.8e-5	9.5E-5	6.2e-6	1.0e-6	1.6e-5	1.1e-4	CPT*

Note: T(15) stands for Taylor (2015), and M(16) for Markham et al. (2016b)
* Robertson (2010) correlation for unit weight. Idriss and Boulanger (2008), Kulhawy and Mayne (1990) and Jamiolkowski (1991) correlations with weights of 0.4, 0.3, and 0.3, respectively for D_r. McGann (2013) correlation for shear wave velocity (V_s) to get G_O. CPT-FC correlation from Robinson (2013) and then FC-e_{max} and FC-e_{min} data from Taylor (2015). Robertson (2015) for hydraulic conductivity.
** Range of D_r and G_O considered for sensitivity analyses is provided for these soils.
*** Parentheses indicate values calibrated against laboratory-based curves

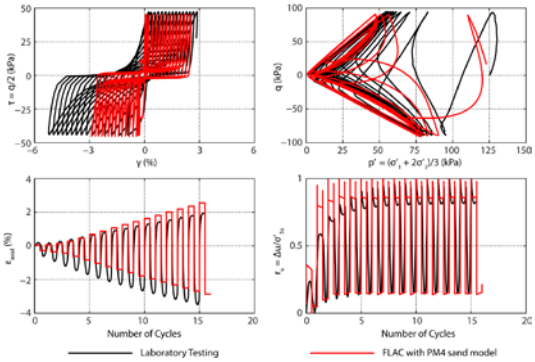

Figure 2. Comparison between laboratory cyclic triaxial test results (black) and FLAC simulated test (red) for a specimen from a depth of 10.97 m at the FTG-7 building site.

3 BUILDING AND SITE DESCRIPTIONS

3.1 CTUC Building

The CTUC office building (S43.529 E172.642) was a 6-story (21-m high) RC frame structure, which was 20 m wide (EW) and 25 m long (NS), supported on individual footings connected with tie beams (Zupan 2014). The building foundation and the eastern NS-oriented structural frame are shown in Figure 3. A majority of the foundation consisted of 2.44-m square footings that were embedded 0.46 m or 0.6 m, which supported 0.5-m wide square RC columns. There were also a large 9-m square footing where two columns, the elevator, and stair core were founded on the west side of the building, a 0.9-m thick, 1.3-m wide, and 15.44-m long EW-oriented footing, which supported a RC block wall, on the north side of the building, and two 0.46-m thick, 0.91-m wide, and 4.88-m long footings that supported southern 0.45 m x 1.5 m RC columns. RC tie beams (0.3 m x 0.38 m) connected the NS-oriented structural frames. In the NS direction, RC tie beams of the same dimension connected the three southern spans, whereas 0.61 m x 1.22 m RC tie connected the two northern spans. The embedment depths of the footings were 1.2-1.3 m. The spacing between columns was 4.9 m to 5.2 m in the NS direction and 9.15 m in the EW direction. The columns of the building had a square section with a width of 0.5 m from ground level to the third floor, where they transition to 0.45-m wide square

columns to the 5th story. The columns were connected on each floor with 0.4 m x 0.6 m beams in the EW direction. In the NS direction, only the eastern frame was connected through beams of the same size. The floor consisted of 0.075-m thick uni-span precast concrete floor with 0.075-m thick RC topping. The top floor was a composition of four EW oriented steel frames connected in the NS direction with steel beams. Footing pressures, including dead load and 20% of the live load, were estimated to be 190–250 kPa.

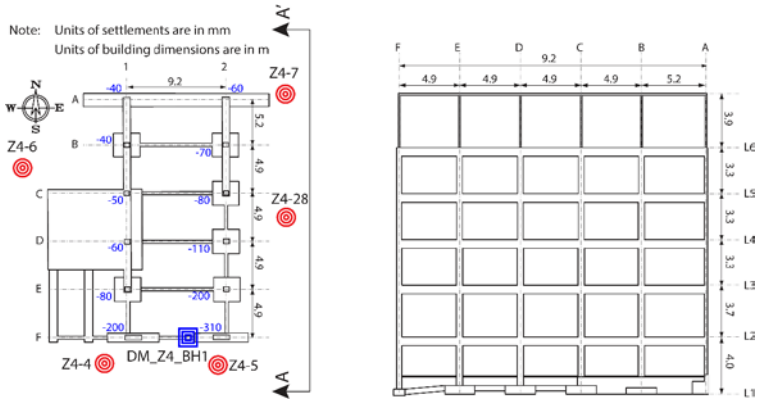

Figure 3. Foundation plan view of the CTUC building and elevation view of its eastern NS-oriented frame.

Six CPTs and one soil boring were advanced to characterize subsurface conditions. The groundwater depth was estimated to be 2.5 m (New Zealand Geotechnical Database 2016). There is fill at the surface which is underlain by a shallow silty sand/sandy silt (SM/ML) layer that extends down to a depth of 2.5 m across the site, except for at the building's south side where this layer extends to 5 m depth. Its CPT tip resistance (q_t) is generally less than 5 MPa ($D_r \approx 35$ - 45%), and its Soil Behaviour Type Index (I_c) is generally between 2.2 and 2.4. A dense gravelly sand with q_t values of 20-30 MPa ($D_r \approx 80$-90%) underlies the shallow SM/ML layer and extends to 7.5-9 m depth. The gravelly sand is underlain by a medium dense sand and silty sand with q_t values of 10-20 MPa ($D_r \approx 60$-70%) and I_c values of 1.6-1.9 which extends down to a depth of 16-17 m. A dense sand soil layer with q_t = 25-30 MPa ($D_r \approx 80$-90%) and I_c = 1.6-1.8 is below a depth of 16-17 m and extends down to 21 m. An overconsolidated silty clay ($I_c > 2.6$ and s_u = 100-200 kPa) underlies this unit down to a depth of 21 m to 24 m. The dense Riccarton Gravel unit underlies the clay unit.

Damage to the CTUC building was negligible during the Darfield earthquake. Severe liquefaction in the foundation soils during the Christchurch earthquake induced differential settlements that produced structural deformation and cracking (Bray et al. 2014). Figure 3 shows measured differential settlements in each column relative to the adjacent building to the north, which did not appear to settle relative to the surrounding ground. The SE column settled significantly more than the other columns. The differential settlement led to angular distortions of 1/50 in the southern span. Large amounts of sediment ejecta were observed at the SE corner of the building and limited ejecta occurred at the column directly north of the SE column. The static bearing capacity factor of safety of the SE column was less than one using the residual undrained strength of the liquefiable sand (Bray et al. 2014).

3.2 **FTG-7 Building**

The FTG-7 building (S43.526 E 172.638) was also demolished after the Canterbury earthquake sequence. It was a 7-floor (23.9-m high) steel frame structure, which was 29.1 m wide (EW) by 31.8 m long (NS), that was supported on reinforced concrete (RC) strip footings (Zupan 2014). Figure 4 shows the foundation plan view with the CPT locations and also a typical interior frame of the structure. In the NS direction, the foundation consisted of two perimeters RC strip footings, which were 0.6 m thick, 2.4 m wide, and 29 m long, with an embedment depth of 1.2 m. The four interior RC strip footings were 0.6 m thick, 3.3 m wide, 25 m long, and embedded 0.6 m into the ground. The distances between the centerlines of the NS-oriented footings and columns were between 5.5 m and 6.3 m. The interior and perimeter footings were interconnected in the EW direction through 0.6 m by 0.6 m RC tie beams. The EW-oriented perimeter footings were 0.6 m thick, 2.0 m wide, 34 m long,

and embedded 1.2 m. The EW perimeter footings were connected to the NS-oriented footings through 0.6 m by 0.6 m tie beams. The distances between the centerlines of the EW-oriented tie beams and columns were between 6.0 m and 6.8 m. The columns were wide-flange steel sections with their web aligned parallel to the NS direction. The dimensions of the *W* sections depend on the building floor and column location. Primary beams connected columns in the NS direction. Secondary beams connected columns and primary beams in the EW direction. The size of the beams depends on the building floor and whether is an interior or perimeter beam as shown in Figure 4. The ground floor consisted of a 0.1-m thick unreinforced concrete slab, and floors 2 through 7 consisted of 0.12-m thick RC slab over 0.75 mm galvanized steel decking. The pressure at the base of a representative footing was estimated to be 80–100 kPa, which includes 100% of the dead load and 20% of the live load.

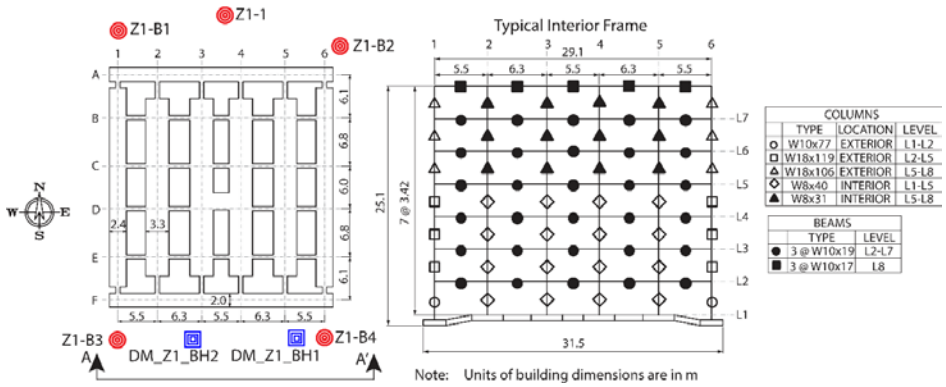

Figure 4. Foundation plan view of the FTG-7 building and elevation view of a typical interior frame.

Five CPTs, which were located near the building corners and along its northern perimeter, and three soil borings, which were located along its southern perimeter, were used to characterize the subsurface conditions at the FTG-7 site. The site conditions are not as variable as typically found in Christchurch. There is fill with relative density (D_r) ≈ 65% from the ground surface to 1-1.5 m depth. A sandy silt/silty sand unit with variable fines content (FC) and soil behaviour type index (I_c) generally between 2.2–2.4 underlies the fill and extends to a depth of 7–8.5 m. The "clean sand" equivalent relative density for this deposit is 35-55%. Below this layer, a medium dense sand (I_c ≈ 1.8 and 2.1) with D_r ≈ 60–70% is found that extends down to a depth of around 14-16.5 m. Below the medium dense sand, very dense sand (D_r ≈ 90%) is encountered. A 1–2-m thick clayey silt (ML/MH) layer with some peat overlies the Riccarton Gravel. The groundwater table depth was about 2.0 m (New Zealand Geotechnical Database 2016).

The seismic performance of the FTG-7 building was assessed in the reconnaissance efforts after several of the key earthquakes as well as detailed floor-level and verticality surveys and LiDAR data performed after the Christchurch earthquake (Bray et al. 2014, and M. Jacka personal communication). There was only minor surficial evidence of liquefaction at the site after the Darfield earthquake. The Christchurch earthquake caused severe liquefaction at the site, and the building was damaged significantly (e.g., the columns at the ground level were structurally damaged). Floor levels and building verticality surveys (Eliot Sinclair and Partners Limited 2011 and Beca Carter Hollings & Ferner Ltd. 2011) indicated tilting of the building towards the SE. One of the surveys indicated a downward displacement of 100 mm of the SE corner of the building relative to its NW corner. LiDAR data indicate free-field ground settlements, which result from volumetric and sediment ejecta mechanisms, of 300 mm for the Christchurch event. Additionally, LiDAR data indicate building settlements of 400 mm for the Christchurch event.

4 ANALYTICAL RESULTS AND INSIGHTS

4.1 Numerical Models

Figure 5 shows the computational models employed in the dynamic SSI analyses performed in this study. Rayleigh damping of about 0.5% at frequencies between 1.5 to 2 Hz was used (corresponding to

the average between the natural frequency of the building and the mean frequency of the input motion). The maximum element size was one tenth of the wavelength associated to the maximum frequency, which in this case was limited to 15 Hz. The elasticity young's modulus and unit weight of concrete were $2.35x10^7$ kPa and 24 kN/m^3, respectively. The flexural cracking of the structural elements was considered by applying a factor of 0.35 and 0.7 to the inertia of beams and columns, respectively (ACI 318-14, 2014). The elasticity modulus and unit weight of steel used for the analyses were $2.0x10^8$ kPa and 77 kN/m^3, respectively. In elements where the stiffness of the system came from different materials (steel and concrete), an equivalent steel section was estimated such that the actual stiffness and weight of the system was obtained for the analysis. The area and second moment of inertia of the *W* sections were obtained directly from AISC (2014). Beams oriented in the direction of the analysis were modelled considering the contribution to the stiffness of the floor slab by using an effective width following the recommendations of the ACI 318-14 (2014). The distribution of beams in the out-of-plane direction was taken into account by using a typical frame spacing.

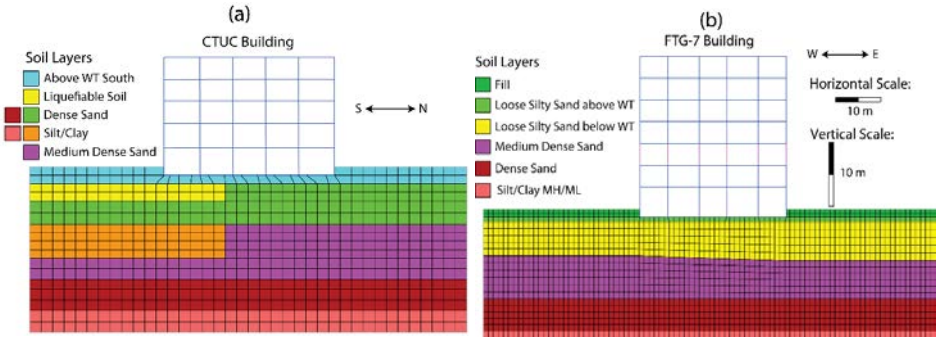

Figure 5. Geotechnical and structural models for the (a) CTUC and (b) FTG-7 buildings.

4.2 **Analytical Results**

The dynamic SSI analyses helped identify the primary mechanisms of building settlement during the Canterbury earthquake sequence (other than sediment ejecta-induced settlement which was not captured in these continuum analyses). The CTUC building performance during the damaging Christchurch earthquake was driven primarily by a bearing capacity-type of failure of the foundations near the SE corner of the building. The SE exterior column is founded on a 4.88 m x 0.91 m spread footing that has loose silty sand/sandy silt just 1.3 m below it. This mechanism led to excessive shear-induced settlements, illustrated by the shear strain contours shown in Figure 6. It is apparent that there is a large concentration of shear strains within the liquefiable soil just below the SE corner of the building. Shear strains on the order of 8% are calculated within the shallow, loose silty sand/sandy silt layer under the SE corner of the building; whereas shear strains on the order of 1-2% are computed within this shallow liquefiable layer in the free-field south of the building. In this area of large shear strains beneath the southern part of the building foundation the soil displaces laterally and upwards. Large shear strains do not develop under the middle and NE corner of the building, because the shallow, loose silty sand/sandy silt was not present below the groundwater table at these locations. The differing responses of the soils directly beneath the shallow foundations of the CTUC building are the primary reasons for the 250 mm differential settlement observed across the building.

Shear strain contours calculated in the soils beneath the FTG-7 building after the Christchurch earthquake are shown in Figure 7(a). The dynamic SSI analyses calculate large shear strains at the edges of the buildings in addition to smaller, but still substantial, shear strains under the building and in the free-field in the loose SM/ML layer found between 2 and 7.5 m depth. A primary mechanism for building settlement in this case is SSI-ratcheting, where the rocking of the building induces high seismic demands in the soils beneath the edges of the building. The rocking of the building is captured in the displacement-time histories calculated at the two exterior columns and one interior column shown in Figure 7(b). In every cycle of shaking as one of the exterior column displaces upward the other exterior column displaces downward, indicating rocking. The interior column displaces steadily downward without the oscillation observed for the exterior columns. The high seismic demands

induced by the building displace the soil laterally from beneath the edges of the building toward the free-field, which produces downward cyclic movement of the building. Consequently, vertical displacements were larger under the exterior columns than under the interior columns. Shear-induced partial bearing capacity and volumetric-induced mechanisms also contributed to building settlement.

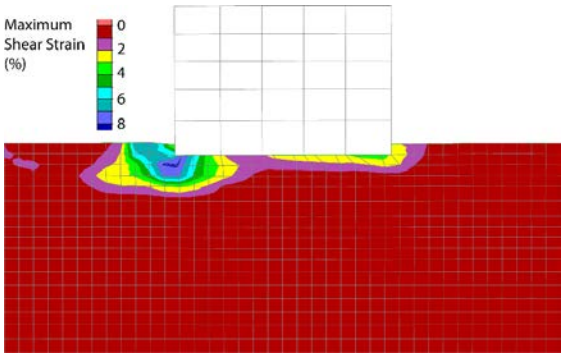

Figure 6. Shear strain contours for soils beneath the CTUC building after the Christchurch earthquake.

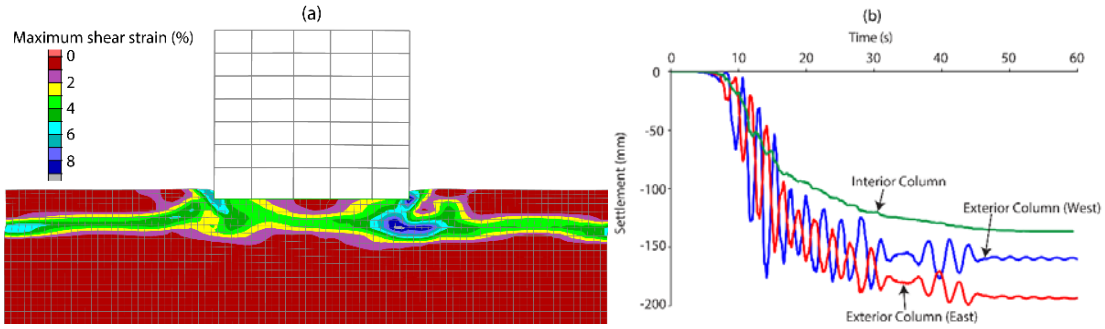

Figure 7. (a) Shear strain contours for soils beneath the FTG-7 building and (b) displacement-time histories at western, eastern, and interior columns for the Christchurch earthquake.

5 CONCLUSIONS

The primary mechanisms of liquefaction-induced settlements of structures are shear-induced, volumetric-induced, and ejecta-induced ground deformation. Dynamic SSI analyses provide salient insights regarding the first two of the key mechanisms contributing to building movements. Building settlement due to shear strains developed in the foundation soils from shaking-induced ratcheting of buildings into cyclically softened soil or from a transient loss of bearing due to soil softening in several cases. Damaging building settlement resulting from volumetric strains in the foundation soils were largely due to liquefaction of shallow soils, if they were present at a site. The dynamic SSI analyses captured these mechanisms of nonlinear soil response. However, the influence of the loss of ground due to the development of sediment ejecta, which was another potentially important factor in some cases, was not captured with this continuum based approach. Engineers should employ simplified procedures and engineering judgment to assess this mechanism. Recommendations for estimating liquefaction-induced building settlement are provided in Bray et al. (2017).

6 ACKNOWLEDGEMENTS

We acknowledge the National Secretary of Higher Education, Science, Technology and Innovation of Ecuador (SENESCYT) and the U.S. National Science Foundation (NSF) through CMMI-1332501 for funding this research. Any opinions, findings, and conclusions or recommendations expressed in this material are those of the authors and do not necessarily reflect the views of NSF or SENESCYT. Collaborations with Prof. Misko Cubrinovski and Dr. Merrick Taylor of the Univ. of Canterbury, Dr. Josh Zupan, Dr. Christopher Markham, and Christine Beyzaei of the Univ. of California, Berkeley, and Mike Jacka of Tonkin + Taylor, Ltd. were invaluable. Discussions with Profs. Ross Boulanger and Katerina Ziotopoulou of UC Davis about the PM4Sand constitutive model were also invaluable.

7 REFERENCES

American Concrete Institute, 2014. Building Code Requirements for Structural Concrete. (ACI 318-14).

American Institute of Steel Construction, 2014. Steel Construction Manual Shapes Database. From: http://www.aisc.org/WorkArea/showcontent.aspx?id=34922, Last accessed: May 16th 2015.

Beca Carter Hollings & Ferner Ltd. 2011. Earthquake Damage Assessment – 151 Kilmore Street. Technical report prepared for Westpark Estates 151 Ltd.

Boulanger, R.W. and Ziotopoulou, K. 2015. PM4Sand (Version 3): A Sand Plasticity Model for Earthquake Engineering Applications. Report No. UCD/CGM-15/01, Univ. of California, Davis, CA; 108 pp.

Boulanger, R.W. and Idriss, I.M. 2016. CPT- Based Liquefaction Triggering Procedures. *J. Geotechnical and Geoenvironmental Engineering*, 142(2), 04015065.

Boulanger, R.W. and Montgomery, J. 2016. Effects of Spatial Variability on Liquefaction-Induced Settlement and Lateral Spreading. *J. Geotechnical and Geoenvironmental Engineering*, 04026086-1.

Bradley, B.A. 2014. Site-specific and Spatially-distributed Ground-motion Intensity Estimation in the 2010-2011 Canterbury Earthquakes. *J. Soil Dynamics and Earthquake Engineering*, 61-62, 83–91.

Bray, J., Cubrinovski, M., Zupan, J., Taylor, M. 2014. Liquefaction Effects on Buildings in the Central Business District of Christchurch. *Earthquake Spectra*, 30(1), 85-109.

Bray, J.D., Markham, C.S., and Cubrinovski, M. 2017. Liquefaction Assessments at Shallow Foundation Building Sites in the Central Business District of Christchurch, New Zealand. *Soil Dynamics and Earthquake Engineering J.*, 92, 153-164.

Dashti, S., Bray, J.D. 2013. Numerical Simulation of Building Response on Liquefiable Sand. *J. Geotechnical and Geoenvironmental Engineering*, 139(8), 1235-1249.

Eliot Sinclair & Partners Limited, 2011. "Ground Floor Levels – 4 March 2011."

Itasca, 2011. Flac – Fast Lagrangian Analysis of Continua, Version 7.0. Itasca Consulting Group, Inc., Minneapolis, Minnesota.

Karimi, Z., and Dashti, S. 2016. Seismic Performance of Shallow-Founded Structures on Liquefiable Ground: Validation of Numerical Simulations Using Centrifuge Experiments. *J. Geotechnical and Geoenvironmental Engineering*, 142(6).

Kulhawy, F.H. and Mayne, P.H. 1990. Manual on estimating soil properties for foundation design. *Electric Power Research Institute*.

Markham, C., Bray, J.D., Macedo, J., Luque, R. 2016a. Evaluating Nonlinear Effective Stress Site Response Analyses using Records from the Canterbury Earthquake Sequence. *Soil Dynamics and Earthquake Engineering*, 82, 84-98.

Markham, C.S., Bray, J.D., Riemer, M.F, and Cubrinovski, M. 2016b. Characterization of Shallow Soils in the Central Business District of Christchurch, New Zealand. *Geotechnical Testing J.*, ASTM, doi:10.1520/GTJ2015024.

McGann, C., Bradley, B., Taylor, M., Wotherspoon, L., and Cubrinovski, M. 2014. Development of an empirical correlation for predicting shear wave velocity of Christchurch soils from cone penetration test data. *Soil Dynamics and Earthquake Engineering*, 75, 15–27.

New Zealand Geotechnical Database, 2016. Funded by the Ministry of Business, Innovation and Employment and the Earthquake Commission, New Zealand. < https://www.nzgd.org.nz> (Aug. 08, 2016)

Robertson, P.K. 2010. Soil behavior type from the CPT: an update. *2nd International Symposium on Cone Penetration Testing, CPT'10, Huntington Beach, CA, USA*. www.cpt10.com

Taylor, M. 2015. The Geotechnical Characterization of Christchurch Sands for Advanced Soil Modelling. Ph.D. Dissertation, University of Canterbury, New Zealand.

Zhang, G., Robertson, P.K. and Brachman, R.W.I. 2002. Estimating Liquefaction induced Ground Settlements from CPT for Level Ground. *Canadian Geotechnical Journal*, Ottawa, 39(5), 1168-1180.

Zupan, J. 2014. Seismic Performance of Buildings Subjected to Soil Liquefaction. Ph.D. dissertation, University of California - Berkeley, Berkeley, CA.